SUPPLEMENTARY ONLINE MATERIAL

Cassini Imaging of Jupiter's Atmosphere, Satellites and Rings

Carolyn C. Porco[1], Robert A. West[2], Alfred McEwen[3], Anthony D. Del Genio[4], Andrew P. Ingersoll[5], Peter Thomas[6], Steve Squyres[6], Luke Dones[1], Carl D. Murray[7], Torrence V. Johnson[2], Joseph A. Burns[6], Andre Brahic[8],Gerhard Neukum[9], Joseph Veverka[6], John M. Barbara[4], Tilmann Denk[10], Michael Evans[1], Joseph J. Ferrier[4], Paul Geissler[3], Paul Helfenstein[6], Thomas Roatsch[10], Henry Throop[1], Matthew Tiscareno[3], Ashwin R. Vasavada[11]

Introduction

The Imaging Science Subsystem (ISS) consists of two framing cameras. The narrow angle camera (NAC) is a reflecting telescope with a focal length of ~2000 mm and a field of view of 0.35°. The wide angle camera (WAC) is a refractor with a focal length of ~200 mm and a field of view of 3.5°. Each camera is outfitted with a large number of spectral filters that, taken together, span the electromagnetic spectrum from 200 nm to 1.1 μm. At the heart of each camera is a charged coupled device (CCD) detector consisting of a 1024 square array of pixels, each 12 μm on a side. The data system allows many options for data collection, including various choices of data compression and on-chip summation.

[1] Department of Space Sciences, Southwest Research Institute, 1050 Walnut Street, Suite 400, Boulder, CO 80302.
[2] Jet Propulsion Laboratory, California Institute of Technology, 4800 Oak Grove Drive, Pasadena, CA 91109.
[3] Department of Planetary Sciences, University of Arizona, 1629 E. University Blvd, Tucson, AZ 85721.
[4] Goddard Institute for Space Studies, NASA, 2880 Broadway, New York, NY 10025.
[5] Division of Geological and Planetary Sciences, California Institute of Technology, 150-21, Pasadena, CA 91125.
[6] Department of Astronomy, Cornell University, Space Sciences Bldg, Ithaca, NY 14853.
[7] Astronomy Unit, Queen Mary, London, E1 4NS, England
[8] C.E. de Saclay, University of Paris, L'Orme des Merisiers, 91191 GIF SUR Yvette Cedex, France.
[9] Department of Earth Sciences, Freie Universitaet, 12249 Berlin, Germany.
[10] Institute for Space Sensor Technology and Planetary Exploration, German Aerospace Center, Rutherfordstrasse 2, 12489 Berlin, Germany.
[11] Department of Earth and Space Sciences, University of California, Los Angeles, CA 90095.

Data collection began on 1 October 2001 with the spacecraft 3.8° above Jupiter's equator plane and approaching the planet from a phase (Sun-Jupiter-spacecraft) angle of 20° and a distance of 84.7 million km. By the middle of November, the phase angle dropped to 18°, and a 2x2 mosaic of images was needed to cover the entire planet. All throughout this period repeated observations of the atmosphere, and satellite searches in the region around Jupiter containing the Galilean satellites occurred.

By the middle of December, the phase angle dropped to 0°, systematic monitoring of the atmosphere ceased, and targeted observations of the rings and known satellites began. After making its closest approach to Himalia, a small outer satellite of Jupiter, on 18 December, Cassini began a sweep through a large range of phase angles during which the ISS monitored the light scattering behavior of the rings and Galilean satellites in a suite of spectral and polarimetric filters. For a brief time surrounding closest approach, Jupiter was large enough to require a 3x3 mosaic to cover the planet.

Ring, satellite and occasional atmospheric observations continued through closest approach and out to 15 January, at which point the spacecraft was looking back on a crescent Jupiter from a distance of 18 million km and 3° below the equator plane. At that time, ISS returned to repeated imaging of the planet as the spacecraft departed. The last Jupiter images were taken on 22 March 2001.

In planning spacecraft imaging sequences, considerations of maximizing the signal/noise of the target often weigh against minimizing smear due to spacecraft jitter. Cassini is a spacecraft whose attitude can be maintained by two mechanisms: the brief firings of hydrazine thrusters (making it like the previous Jupiter-bound spacecraft Voyager and Galileo) or spinning discs called reaction wheels. Together with the large inertia of the massive Cassini spacecraft, reaction wheels make for an extremely stable platform: In stability tests, in which the star Fomalhaut was imaged in September 2000, immediately preceding the Jupiter encounter, the spacecraft maintained its pointing to within 6 μrad for a period of 32 sec. However, the Jupiter imaging sequences were planned before these stability values were in hand, and a smear rate typical of thruster attitude control of 6 μrad/sec - ie, one NAC pixel per second -- was assumed. As a result, the image sequence exposures were shorter than they needed to be, reducing the signal/noise in those circumstances which required long exposures (eg, imaging in the UV where the sun's intensity is low, or atmospheric imaging in the near-IR weak methane bands) and reducing our sensitivity to previously undetected bodies in the images planned for satellite searches around Jupiter.

Nonetheless, the sensitivity and large dynamic range of the CCD detectors permitted the acquisition of a wealth of startlingly clear and detailed images during Cassini's Jupiter flyby. In all, about 26,000 images were collected -- a bounty that is Voyager-class in size.

(Because of an anomaly in the reaction wheel subsystem, the spacecraft was placed on thruster control on 16 December 2000, 00:57 UTC. Between 19 December 10:51 UTC and 29 December 02:00 UTC, data collection ceased entirely while the anomaly was studied. Observations of Jupiter, the rings and satellites planned for this interval, which covered phase angles 12° - 53°, were hence never acquired.)

Jupiter's atmosphere

From 1 October through 15 November 2000, Jupiter's entire disk fit within the ISS NAC field of view. During this time, images were acquired in nine spectral filters (*S1*). Between mid-November and 9 December 2000, a 2x2-image pattern was needed to cover the disk and spectral coverage was reduced to five core filters (*S2*). During both periods, every 72° of longitude was imaged as Jupiter rotated beneath the spacecraft. Coverage of the entire planet -- 360° in longitude -- was acquired once every 20 hours (Jupiter's rotation period is ~10 hr), with an additional 10-hour time step inserted every 5 days.

Convective Clouds. Scatter plots of brightness in three channels (Fig. S1) depict the storm evolution in Figure 3 (main text) more quantitatively. The slopes of the clusters of points in these diagrams are determined by cloud top height and/or optical thickness variations (*S3*). On 2 December, the initial storm appears as a few exceptionally bright pixels at all wavelengths relative to the main cloud layer. By 3 December, after the initial storm dissipates, these pixels are no longer present. By 7 December, at the height of the major convective event, a distinct cloud of points that are bright at all wavelengths appears; the unusually high 889 nm albedos indicate that the convective event penetrates well into the upper troposphere. Since these clouds are optically thick, the steeper slope of these points in the 727-751 nm and 889-727 nm planes, relative to that for the main cloud, is probably due to cloud top height variation. By 11 December, the distributions resemble those on 3 December, but the deep cloud is evident as a horizontal cluster of points that are bright in the continuum but dark in the weak methane band.

Jupiter's north polar stratosphere in the ultraviolet. Previous studies of Jupiter's polar regions (*S4 - S15*) indicated the presence of small (sub-micron) particles or aggregates of small particles (*S16*) in the polar regions, composed of complex hydrocarbons, the end products of hydrocarbon chemistry initiated by the breakup of methane due to energetic auroral electrons and protons (*S8 - S10*). Vincent *et al.* (*S11*) found contrast patterns appearing to be stationary in a coordinate system rotating with system III longitude, the same frame that controls the auroral morphology. For these reasons, the Imaging Team was interested in investigating the jovian polar regions in the UV.

The movie (Movie S2) captures the formation in early October of a large dark oval, about the size and shape as Jupiter's Great Red Spot, when it first appeared as an enlargement at the east end (longitude 180°) of long narrow dark channel extending from longitude 180° to 240° near the 60° latitude circle. At that time, only the eastern third of the feature fell on or near the main auroral oval.

By 13 October 2000 (Fig. S3b) the enhancement at the east end became larger and darker and the tail trailing to the west along the 60° latitude circle became smaller and less distinct. The dark oval continued to grow and move to the east, mostly inside the auroral oval by 29 October; by that time, the thin feature extending toward the west was almost invisible. The center of the oval moved from longitude 180° to 170° by 13 November (Fig. S3d) and a brighter inner core region appeared at that time. Its boundary on the equatorial side closely followed the shape of the auroral oval in mid-November. The feature, as it appears in Fig. S3d, is similar in size, shape, and longitude to a feature seen in 1997 HST images (*S17, S18*). The movie shows the outer portion of the dark oval circulating in a clockwise sense while features within the larger polar vortex defined by the 60° latitude circle are circulating in the counter-clockwise (prograde) sense. During this time, it changes shape rapidly, evolving toward the more elongated structure seen in Fig. S3f on 13

December, by which time it has moved out of the auroral oval, elongating in longitude from ~ 45° to 135°, but with a diminished latitudinal extent. Almost half the feature at that time extended south of the 60° latitude circle. A smaller dark region formed closer to the pole near longitude 90°. Other frames show this spot shearing and moving to lower longitudes (in the prograde direction) as do the other contrast features within the circumpolar vortex poleward of 60° latitude.

Jupiter's aurorae: On each of 8, 13, and 20 January 2001, ninety NAC images were taken of the planet in several different filter combinations. Scattered light from the bright crescent, which fell in the field of view, made the aurora indistinct in most of them; it was clearly visible in 34 images. Of these, there were 10 aural images that also contained stars to help determine the camera pointing. The aurora appeared brightest - with the greatest contrast relative to the scattered light background - in the Hα (HAL) filter centered on 656 nm. This line of atomic hydrogen is expected to be prominent in Jupiter's hydrogen-helium atmosphere (*S19*). The aurora also appeared visible, though less clearly, in the red and green filters (*S20*).

Galilean satellites

Eclipse results. Io was the best studied of the satellites, with more than 500 NAC images taken during 4 eclipses, 3 of which were successfully recorded. Previous Io eclipse imaging by Galileo (*S21*) had shown colorful optical emissions on Io, but Galileo was not able to capture temporal variability, and the identity of the emitting species was not known. With its high data rate and numerous filter combinations, Cassini was able to fill some of the gaps in our knowledge of Io's visible aurorae and their temporal variations (Fig. S4; Movie S3).

Europa was observed during an eclipse on 10 Janaury 2001; the satellite could still be detected in clear filter images more than an hour after ingress. Moonlight from Ganymede could account for much of the signal observed during this event, though atmospheric emissions of at least 10 kR were detected along Europa's limb. Figure S5 shows that the limb of Europa was brighter than the center of the disk, opposite to the behavior expected from reflected moonlight, and also shows a local concentration of emission in the northern hemisphere of the Jupiter-facing side of Europa. Similar limb-brightening and spatial heterogeneity were observed in HST/STIS oxygen images of Europa in the far-UV (*S22*).

An eclipse of Ganymede was recorded on 11 January 2001, revealing a thin crescent on the Jupiter-facing (sunward) side, probably due to illumination by light scattered from aerosols in Jupiter's upper atmosphere. No obvious equatorial glows were detected.

Cassini images of Io revealed 2 giant plumes: Pele, and a newly-discovered plume over the north pole later found to be associated with Tvashtar volcano (Fig. S6).

Small satellites

Himalia. Himalia is a member of the prograde group and has a semi-major axis of 11.4 million km and a period of 251 days. It is the largest of all outer Jovian satellites and the second largest "non-Galilean" satellite of Jupiter after Amalthea, with radius ~ 88 km). Cassini ISS obtained four

multi-color image sequences of Himalia, each separated by ~1.5 hr, over the wavelength range of 0.3 to 1.0 μm (93 images in total). Almost exactly 1/2 rotation was captured, if the spin period of 9.5 h (*S23*) is correct. The flyby distance of 4.44 million km gave an image scale of 27 km on the surface. This was the closest approach of Cassini to any known object in the Jovian system. The phase angle was 70° for all observations.

Metis and Adrastea. Metis was captured in a series of movie images of the jovian main ring (movie S4) shuttered during 11, 12, and 13 December at low phase, in another movie series taken during 15 and 16 January at high phase, and in a small number of images taken during Cassini's crossing of the ring plane on 31 December. Adrastea was seen in both the low phase (mid-December) and high phase (mid-January) movie sequences, though with great difficulty in the latter. These movie sequences allowed frequent sampling of the satellites' motions and consequently the shapes and inclinations of their orbits. Additional Adrastea images were obtained on 6 January. In total 56 ISS images of Metis and 27 of Adrastea were used in the fit which entailed fitting precessing ellipses directly to the observations using a weighted least squares differential correction technique.

Satellite searches. The spacecraft's distance to Jupiter for the satellite search images ranged from 82 million km to 25 million km, and the phase angle ranged from 20° to 8°. Due to limitations on observing time on the spacecraft, image sequences (1x4 NAC image mosaics on either side of Jupiter) were taken at intervals ranging from many hours to days. The translational movement of the spacecraft through the encounter, as well as the movement of any observed satellites, over these intervals was so large as to make it impossible to identify objects by the usual method of observing their motion against a background of stars. Instead, a correlation technique was applied, which restricted the search to satellites with near-planar, near-circular orbits. Along with the usual albedo/size limits placed on unseen objects, these assumptions placed additional limits on the orbital elements of any detectable satellite.

Apart from the four Galilean satellites, which were frequently visible and saturated the detector, the Jovian satellite Thebe was also detected in 3 image pairs. The processing routines successfully identified Thebe as a candidate object in all three cases; however, the correlation routine failed to identify Thebe as a moon because its eccentricity is higher than the maximum eccentricity assumed by the correlation technique.

Rings

The ISS Jupiter ring observations consisted of ~1200 targeted images of the Jovian ring system, taken over 37 days. They included two 40-hour movies of the ring on the inbound leg (phase ~ 0.5°-2.5°; Movie S4) and outbound leg (phase ~ 120°); observations while crossing through the ring plane, with phase 60° – 75° and spacecraft latitude </~ 1°); a search for new faint rings; and multi-band (λ = 0.31 - 0.91 μm) and polarimetric imaging at phase angles ranging from near 0° to 120°. (A portrait of the jovian ring over a range of phase angle and distance as seen by the Cassini ISS is shown in Fig. S7). Cassini's closest approach distance of 136 R_J was significantly farther than that of Voyager (5 R_J) or Galileo (10R_J), and thus the maximum spatial scale in the NAC was coarser: only ~ 58 km/pixel. Most exposures were less than three seconds to minimize smear due to the then-uncharacterized pointing stability of the spacecraft.

The main ring was detected in nearly all targeted exposures. The extreme scattered light environment so close to Jupiter (angular separation ~ 0.5º) required short exposure times, resulting in the ring being just above the detection limit in many images. This is particularly true for those images taken early in the flyby when the angular separation between ring and planet was at a minimum and the planet's lit hemisphere scattered light into the camera optics.

The halo and gossamer rings were not detected in any images. Both of these jovian ring components are fainter than the main ring, which put them below our detection threshold. For the same reason, searches for new faint gossamer rings out to 6 R_J, well beyond the locations of the known Thebe and Alamthea gossamer rings, were negative. Measurements of the ring's polarization are currently inconclusive for similar reasons.

The main ring was seen near ring plane crossing (phase ~ 65º). The derived ISS constraint on vertical thickness of $z < 300$ km improves neither on the Voyager-era constraint of $z < 30$ km in backscatter nor on a more recent Galileo side-scatter thickness of $z \sim 100$ km. We sought brightness variations in ring azimuth that might indicate the presence of 'spokes' or 'clumps' of material due to recent events in the ring. However, we were unable to discern any longitudinal or temporal variation in the ring's brightness at spatial scales larger than that of the images: 50 – 120 km/pixel. Better modeling of the scattered light structure is needed to derive any further constraints on ring structure or temporal variability than those reported here.

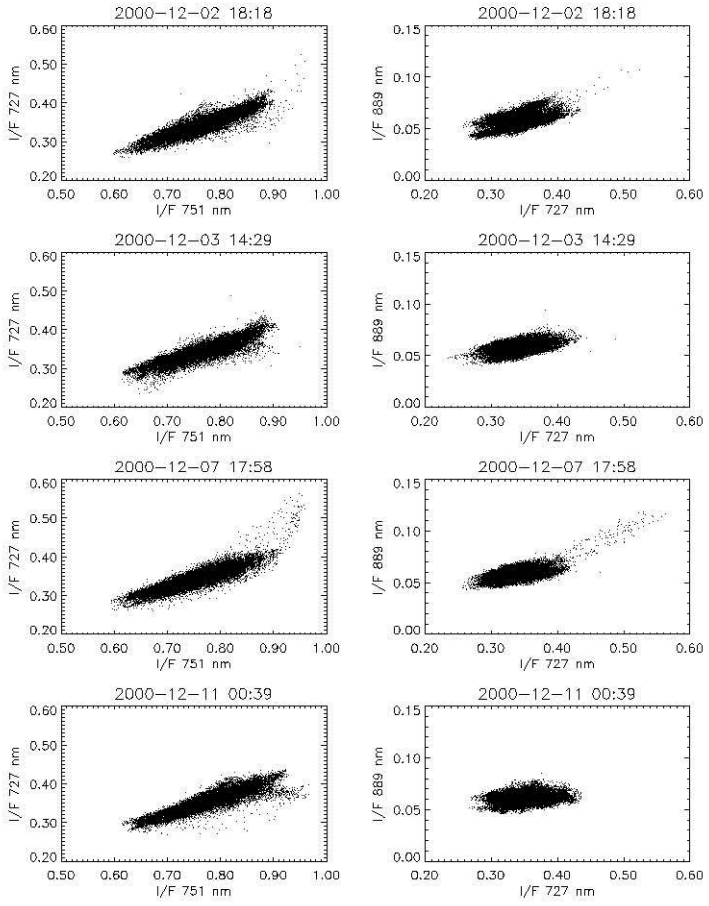

Figure S1. Scatter plots of weak methane band (727 nm) vs. continuum (751 nm) albedo (left panels) and strong methane band (889 nm) vs. weak methane band albedo (right panels) during the evolution of the storm in Figure 3. First row: 2 December, 18:18. Second row: 3 December, 14:29. Third row: 7 December, 17:58. Fourth row: 11 December, 00:39. All times are UTC.

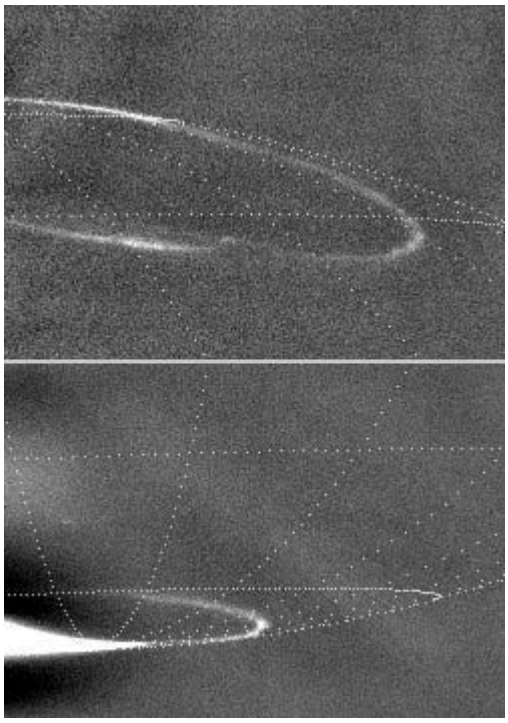

Figure S2. NAC images taken of the northern and southern aurora on 13 January 2001 in the Hα filter when the spacecraft was approximately 16.5million km from the planet and about 2.5° below the equator. The smallest features are about 100 km across. The images, taken 13 hours apart, have been processed to remove scattered light from the overexposed crescent of the planet. Jupiter's magnetic rotation axis is tilted relative to the rotation axis and offset from the center of the planet, so the magnetic pole is offset from the rotational pole in the north but more closely coincident with the rotational pole in the south. These Cassini imaging observations are the first to capture Jupiter's southern aurora on the planet's night side.

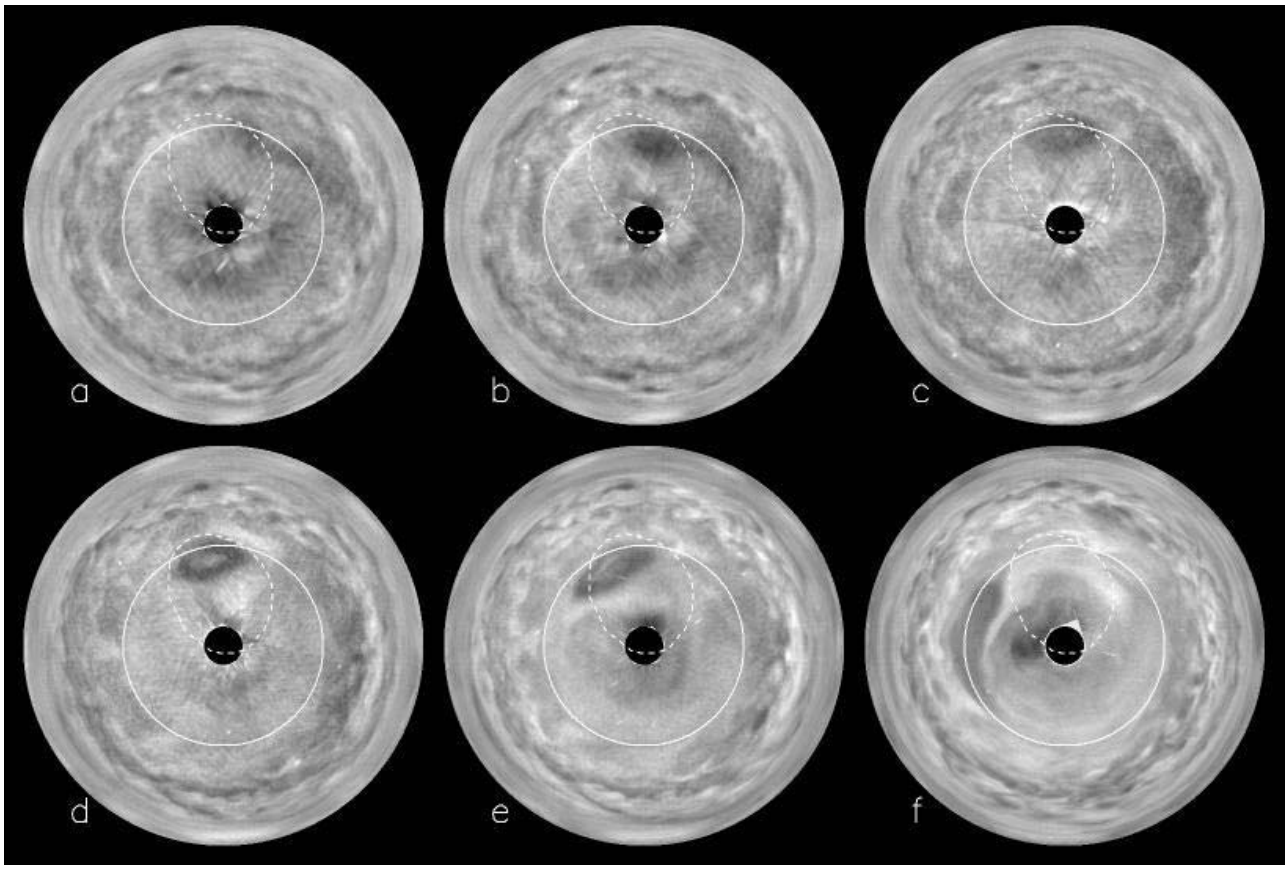

Figure S3. Six different views of Jupiter's northern hemisphere seen in the ultraviolet over the course of 10 weeks. Each is a composite of six or more 2x2 summed UV1 (258 nm) NAC images taken over one Jupiter rotation. All images were photometrically flattened, map projected to a polar view with the equator at the perimeter, and the result was divided by a longitudinally averaged brightness at each latitude to enhance small-scale contrast. Imperfections in this process produced `seams' visible in some of the mosaics, especially near the pole. The highest latitudes were invisible poleward of ~ 85° latitude. All images were obtained in the year 2000. The date of the last image obtained in each mosaic is: (a) 3 October, (b) 13 October, (c) 29 October, (d)13 November, (e) 20 November and (f) 13 December. The spatial resolution improved as Cassini approached Jupiter between October and December. The zero point of System III longitude is at the bottom of each mosaic, with longitude increasing in the clockwise direction. The 60° latitude circle is shown. The location of the main auroral oval is plotted as a broken curve.

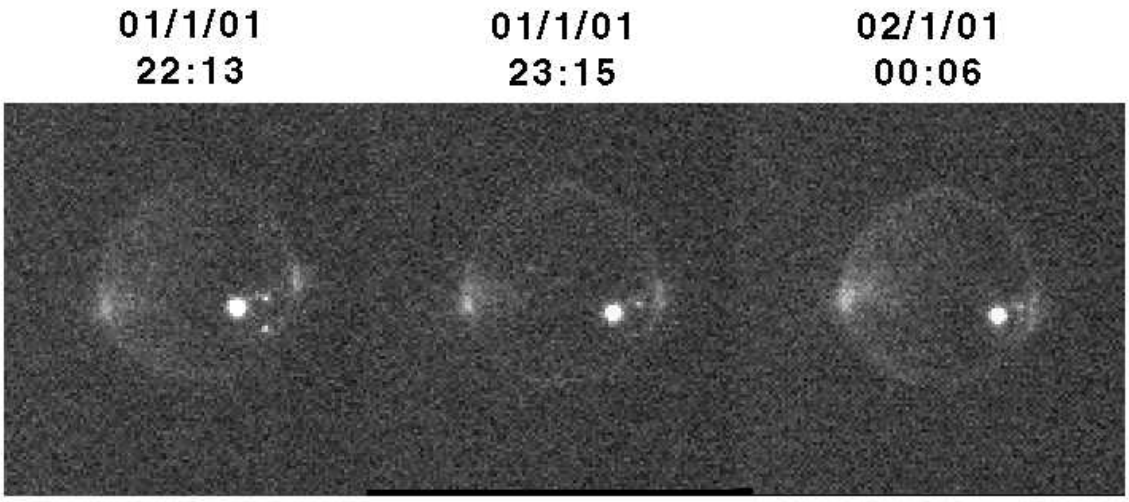

Figure S4. Time-lapse sequence of clear-filter NAC images of Io during the eclipse of 1 January 2001. (See Movie S3).

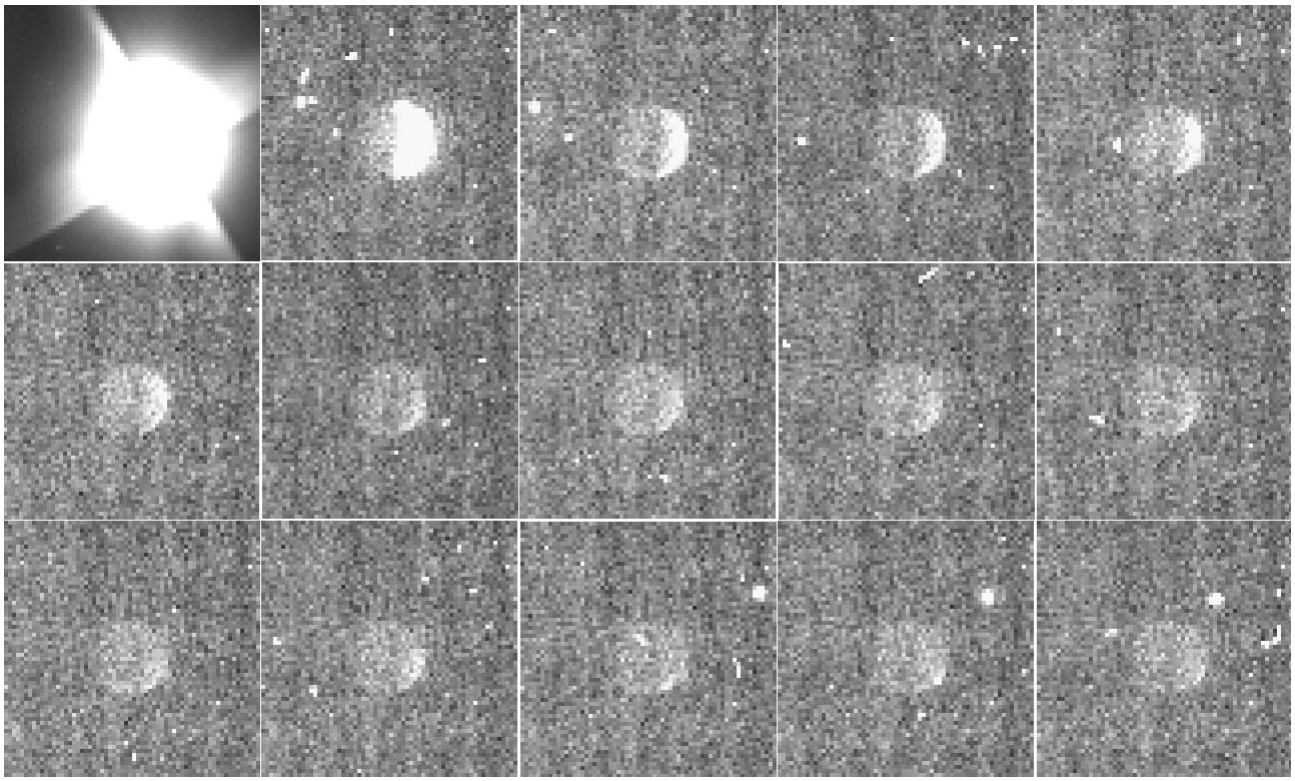

Figure S5. This montage of clear-filter images shows the appearance of Europa during the eclipse of 10 January 2001. The images were acquired at a spatial scale of 85 km/pixel and show Europa's orbital trailing hemisphere, centered on longitude 253W, with north at the bottom and Jupiter towards the right. The imaging sequence spanned more than hour, starting with the upper left image and proceeding to the right and then down through the following rows. Europa traversed the jovian

magnetic equator during this period, as its System III longitude increased from 100 to 151 degrees. The first frame shows Europa overexposed in the penumbra of Jupiter's shadow at 10:36 UTC. The second frame was taken at 10:58 UTC (soon after Europa entered umbral eclipse at 10:53 UTC) and the subsequent images were taken at 5.5 minute intervals, ending at 12:10 UTC. A field star can be seen in the last three frames. Europa was faintly illuminated by moonlight reflected from Ganymede during this eclipse, but the limb-brightening (shown by the ring around the disk of Europa, visible especially during the later observations) indicates atmospheric emissions. Patchy bright emissions can be seen towards the bottom right edge of the disk, at a location near 40N, 345W.

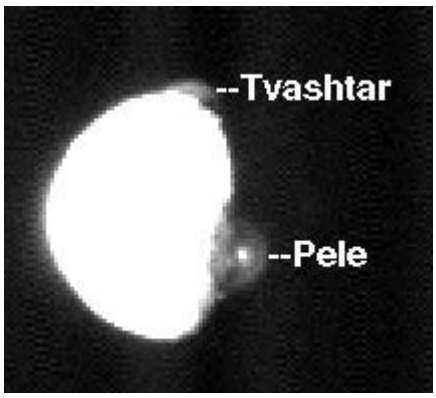

Figure S6. Near-ultraviolet (338 nm) image of Io acquired by Cassini ISS, showing the giant plumes of Pele and Tvashtar. Tvashtar is erupting at 63° N latitude on the opposite side of Io, so only the top 180 km of the 400-km high plume is seen. The top of the Pele plume is illuminated where it projects into sunlight beyond the terminator. Image has been processed to best show the plumes, saturating the illuminated disk of Io, but the digital data is unsaturated. The bright spot at Pele reveals that the plume has a concentrated vertical eruption column.

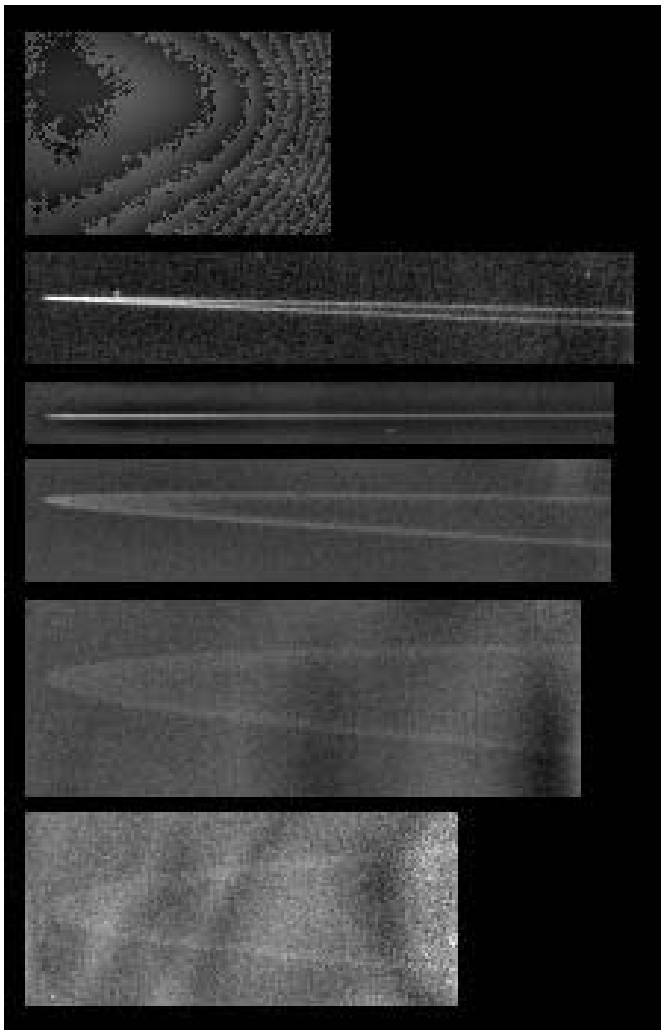

Figure S7. Portrait of the ring through the encounter. All images are of the left ansa, as seen from the spacecraft. Phase angles are 2º, 60º, 64º, 75º, 94º, and 120º. Exposure lengths and filters vary. Observations at the beginning and end (ie, top and bottom) have the lowest resolution and greatest scattered light.

TABLES

Table S1. Images used for Jupiter aurora investigation. The columns are image number, the time of observation, the west longitude of the spacecraft and of the Sun, and the filters used for each image: RED (650 nm), GRN (568 nm), and HAL (Hα 656 nm). The latitude of the Sun decreased from 2.89° to 2.86° during these observations. The `colors' refer to the plotted data points in Figure 6 in the main text.

Image Number	SC Lat	SC Long	Sun Long	Filters
Orange triangles	(2014h UT 08 Jan 2001 - 2054h UT 08 Jan 2001)			
n1357676794	-2.47558	218.87901	322.86689	HAL
n1357679058	-2.47968	241.51693	345.67494	RED
n1357679131	-2.47981	242.24978	346.41040	GRN
Red stars	(0922h UT 13 Jan 2001 - 0924h UT 13 Jan 2001)			
n1358069660	-2.99680	205.25643	320.71317	RED
n1358069733	-2.99687	205.99021	321.44863	GRN
Green squares	(1922h UT 13 Jan 2001 - 2008h UT 13 Jan 2001)			
n1358105660	-3.02971	207.11796	323.38687	RED
n1358108118	-3.03188	231.82610	348.14931	HAL
n1358108360	-3.03210	234.25886	350.58740	RED
Pink crosses	(023h UT 20 Jan 2001 - 1025h UT 20 Jan 2001)			
n1358678192	-3.36826	205.43269	331.21888	HAL
Blue crosses	(2053h UT 20 Jan 2001 - 2054h UT 20 Jan 2001)			
n1358715958	-3.38226	225.43914	351.68242	HAL

REFERENCES:

S1. GRN (568nm), CB1 (619nm), CB3 (938nm), MT1 (619nm), and those in S2.
S2. UV1 (258nm), BL1 (451nm), CB2 (751nm), MT2 (727nm), and MT3 (889nm).
S3. D. Banfield *et al.*, *Icarus* **135**, 230 (1998).
S4. M. G. Tomasko, R. A. West, N. D. Castillo, *Icarus* **33**, 558 (1978).
S5. P. Smith, *Icarus* **65**, 264 (1986).
S6. M. G. Tomasko, E. Karkoschka, S. Martinek, *Icarus* **65**, 218 (1986).
S7. R. Wagener, J. Caldwell, *Icarus* **74**, 141 (1988).
S8. C. W. Hord *et al.*, *Science* **206**, 956 (1979).
S9. R. A. West, *Icarus* **75**, 381 (1988).
S10. W. R. Pryor, C. W. Hord *Icarus* **91**, 161 (1991).
S11. M. B. Vincent *et al.*, *Icarus* **143**, 205 (2000).
S12. A. Sanchez-Lavega, R. Hueso, J. R. Acarreta, *Geophys. Res. Let*. **25**, 4043 (1998).
S13. K. Rages, R. Beebe, D. Senske, *Icarus* **139**, 211 (1999).
S14. R. A. West, M. G. Tomasko, *Icarus* **41**, 278 (1980).
S15. D. Banfield *et al., Icarus* **134**, 11 (1998).
S16. R. A. West, P. H. Smith, *Icarus* **90**, 330 (1991).
S17. M. B. Vincent *et al.*, *Icarus* **143**, 205 (2000).
S18. Several HST images were used to measure polar stratospheric winds and differences were found when compared to tropospheric winds (*S17*). One of us (West) found a UV-dark oval near planetocentric latitude 60° having about the same size and shape as Jupiter's Great Red Spot in an HST image obtained in 1997 in a filter with the same spectral characteristics as the UV1 filter on the ISS NAC. It was not seen in other UV images from HST taken on average. once or twice per year between 1994 and 1999, although not all images have been examined closely. Therefore, prior the Cassini encounter it was thought that this type of feature was rare or perhaps a singular event .
S19. W. J. Borucki, C. P. McKay, D. Jebens, H. S. Lakkaraju, C. T. Vanajakshi, *Icarus* **123**, 336 (1996).
S20. A.P.Ingersoll *et al., Icarus* **135**, 251 (1998).
S21. P. Geissler *et al., Science*, **285**, 870 (1999).
S22. M. McGrath *et al.*, paper presented at the 32nd Annual Meeting of the Division of Planetary Sciences, American Astronomical Society, Pasadena, CA, October 2000.
S23. J. Degewij *et al., Icarus* **44**, 520 (1980).